

Migrating sparse-receiver data for AVO analysis at Teal South Field

Guy Purnell*, Dwight Sukup, Joe Higginbotham, and Dan Ebrom, *Texaco*

Summary

In processing a 3-D ocean-bottom-cable (OBC) survey from Teal South Field in the Gulf of Mexico, we had to address unusual challenges to imaging and AVO analysis. Sources were located on a dense grid, but the receiver grid consisted of only 24 widely spaced locations. In processing the survey, we obtained the best results by applying conventional AVO preprocessing followed by prestack migration (of common-receiver gathers). In comparing prestack and poststack migrations of the survey, we found that for bright-spot analysis and structural interpretation, migration after stack is sufficient. However, comparison of unmigrated and migrated CMP stacks makes it clear that AVO analysis should be preceded by migration. The common practice of comparing limited-range stacks (with migration either before or after stack) conveys some useful information, but is also complicated by acquisition footprint effects, especially in the near-range data. The common-receiver migration provided imaged anomalies that are stronger, more sharply defined, and more consistent spatially with fault-bounded reservoir compartments. It also provided 24-fold image gathers that we input to linearized AVO inversion. A resulting fluid-factor volume highlights AVO anomalies that are consistent with well control and with structure and bright spots known from a previous 3-D streamer survey.

Introduction

Modern 3-D seismic surveys typically involve a fairly dense grid of receiver locations. However, there has recently been an increase in the number of surveys being acquired that are source-rich, but receiver-poor (e.g., marine ocean-bottom-cable or "OBC" surveys). Successful exploitation of such sparse-receiver surveys presents additional challenges beyond those normally encountered with conventional marine streamer surveys.

Teal South Field is located in the Gulf of Mexico, 160 miles southwest of New Orleans, where the water depth is about 82 m. Oil is produced from unconsolidated Tertiary sands at depths in the range of 1200-2400 m. In 1997, an OBC survey was recorded at Teal South (Ebrom, et al., 1998; Purnell, et al., 1999). In 1999, a repeat survey was recorded for "time-lapse" comparison.

In this paper, we use the 1997 survey to investigate whether useful AVO analyses can be conducted using such sparse-receiver surveys. Further, we seek to develop a reliable methodology for preprocessing the data for AVO analysis.

We think the following questions are important: (1) In view of the sparse receiver grid, will it be possible to exploit static AVO information from a single 3-D survey? (2) Will we have to modify or abandon our preferred processing approach for sparse-receiver surveys in order to exploit AVO effects?

Survey design

For the 1997 survey, receivers were deployed in a static ocean-bottom grid, consisting of 24 4-C receiver groups along four east-west cables (Fig. 1). Each cable contained six receiver groups spaced 200 meters apart (east-west). The cables were spaced 400 meters apart (north-south). Sources were deployed on a 3x3-km grid, with planned source spacing of 25 m, in-line and cross-line (Fig. 1). The source was a small airgun array towed at a depth of 3 m.

Data processing

The geometry of the 1997 survey is akin to that of a vertical-cable survey (e.g., Krail, 1994) reduced to having only one receiver level. Our approach to processing such surveys involves 3-D prestack migration of common-receiver gathers. In this, we assume source-receiver reciprocity and apply a PSPI algorithm for 3-D shot-record migration.

However, for this study, we did have to modify our vertical-cable processing methodology. In previous projects, it was oriented toward structural imaging, without any particular concern for preserving amplitude relationships. For the Teal South OBC surveys, we decided to use the hydrophone component to test ways to extend this processing methodology to amplitude analysis of all four components. Specifically, we applied conventional AVO-preprocessing steps to the hydrophone component of the survey, applied 3-D prestack migration, then evaluated the results. The additional preprocessing steps included offset-dependent wavefront spreading correction, Q compensation, and several surface-consistent steps (amplitude compensation, predictive deconvolution, and residual statics).

How well do we sample and preserve AVO responses?

Before attempting to draw conclusions from the processing results, we wanted to understand to what extent the acquisition geometry and/or the migration process might introduce unwanted distortions of the subsurface AVO response.

Using sparse-receiver data for AVO

First, we examined the effects of irregularities in the distribution of sources and receivers (Figure 1). On the scale of seismic wavelengths, the source grid is dense and the subsurface is likely to be adequately illuminated. However, maneuvering of the source boat to avoid obstacles did result in gaps, some of which are significant. If we are to apply our prestack migration approach, we must apply some means to regularize the input common-receiver gathers so that they consist of traces on a regular spatial grid, without distorting amplitude relationships. To this end, we devised a regridding procedure that performs local polynomial fitting to data that are irregularly located in both horizontal coordinates.

The receiver grid, on the other hand is quite sparse, and we cannot compensate for it by binning or interpolation. We examined the distribution of azimuths and offsets in CMP bins and found them to be limited and highly variable spatially. In previous structural imaging projects, the effect of such sparsity has been mitigated by the density of the source grid. However, this may still pose a problem for amplitude studies.

Next, we used synthetic data to investigate how well the migration process preserves recorded AVO effects. We found that amplitude behavior in the input data was preserved in the output images, except near the survey edges. This appears to be a data-truncation effect associated with the finite shot grid, rather than an artifact of the migration algorithm. Since we could forward-model this effect at each depth, we tested the notion of compensating the output images for the predicted edge-of-data effect, using a simple amplitude-weighting scheme. The compensation worked well on synthetic data. On the real data, it ultimately had little effect, except for accentuating acquisition-footprint effects near the edges of the survey.

Discussion of results

Our first check on the processing results was to compare the image volume obtained by stacking the prestack-migrated data to the corresponding volume produced by poststack time migration of a CMP stack of the data. The two volumes agree quite well in their delineation of fault blocks and hydrocarbon-related amplitude anomalies that terminate at fault-block boundaries. Further, they also agree with 3-D migrated stacks of earlier streamer data and with well control. For bright-spot analysis and structural interpretation, migration after stack appears to be sufficient.

In an unmigrated CMP stack of the data, hydrocarbon-related bright spots are unfocused and extend beyond the fault-block boundaries known to separate productive and non-productive occurrences of the same sand. For prestack

amplitude analysis, therefore, it is clear that prestack migration beforehand is necessary if anomalies are to be interpreted at the correct locations.

We applied poststack time migration to near-, mid-, and far-range CMP stacks (Figure 2), and found that this conventional approach to 3-D amplitude analysis was useful for identifying normal-incidence bright spots and AVO anomalies in their correct locations. However, possible artifacts of the sparse-receiver geometry are most conspicuous on the migrated near-range stack. Estimating the AVO gradient by subtracting a near-range stack from the far-range stack may well result in a difference volume that is also contaminated by footprint effects.

We also created near-, mid-, and far-range stacks of the image traces from the common-receiver migrations (Figure 3). The results are consistent with those obtained from migrating the limited-range CMP stacks, although the anomalies stand out more from the background amplitudes and seem to be better focused.

If such estimates of near-, mid-, and far-range reflectivity were completely reliable, it might be sufficient to apply poststack migration to limited-range (or limited-angle) stacks. However, we hypothesized that AVO inversion of the unstacked output of prestack migration was more likely to yield AVO attributes representative of the actual angle-dependent reflectivity. In particular, we hoped that applying relatively robust line-fitting to parameterize AVO in the 24-fold image gathers would be superior for estimating attributes (e.g., compared to simply subtracting far- and near-angle volumes to estimate the AVO gradient).

An AVO attribute that we found useful at Teal South is the fluid factor (Smith and Gidlow, 1987). When calculated after prestack migration, the fluid factor anomaly (Figure 4) associated with one of the productive sands facilitates interpretation of the extent of the pay and its terminations updip (against the fault) and downdip (at the oil-water contact).

Conclusions

Despite the sparse receiver grid, we were able to obtain AVO attributes from the hydrophone component of the 1997 Teal South 3-D OBC survey that are consistent with well control and with bright spots and structural control from earlier streamer data. We believe that this agreement is because the AVO response of the subsurface was sufficiently well sampled by the survey, and because the sampled response was preserved through the processing sequence. The latter belief is also supported by synthetic-data tests of the PSPI 3-D prestack migration algorithm.

Using sparse-receiver data for AVO

The agreement between images from prestack migration and poststack migration indicates that for bright-spot analysis and structural interpretation, migration after stack is sufficient. However, comparison to the unmigrated CMP stack makes it obvious that if AVO analysis is to be done, some form of prestack migration beforehand is necessary. Migration of limited-range (or limited-angle) stacks appears to be useful and is relatively inexpensive. On the other hand, migration of common-receiver gathers is efficient for surveys of this type and offers a number of advantages. One of these lies in providing image gathers that are well-suited for input to linearized AVO inversion.

If conventional AVO-preprocessing steps are included, our modified vertical-cable processing approach appears to be suitable for both static and time-lapse AVO comparisons using this type of sparse-receiver survey.

References

Ebrom, D., Krail, P., Ridyard, D., and Scott, L., 1998, 4-C/4-D at Teal South: The Leading Edge, **17**, No. 10, 1450-1453.

Krail, P., 1994, Vertical cable as a subsalt imaging tool: The Leading Edge, **13**, No. 8, 885-887

Purnell, G., Nolte, B., Krail, P., and Ebrom, D., 1999, Analysis of 4-C data for AVO effects at Teal South, Eugene Island 354: Offshore Technology Conference, Expanded Abstracts.

Smith, G. C. and Gidlow, P. M., 1987, Weighted stacking for rock property estimation and detection of gas: Geophys. Prosp., **35**, no. 09, 993-1014.

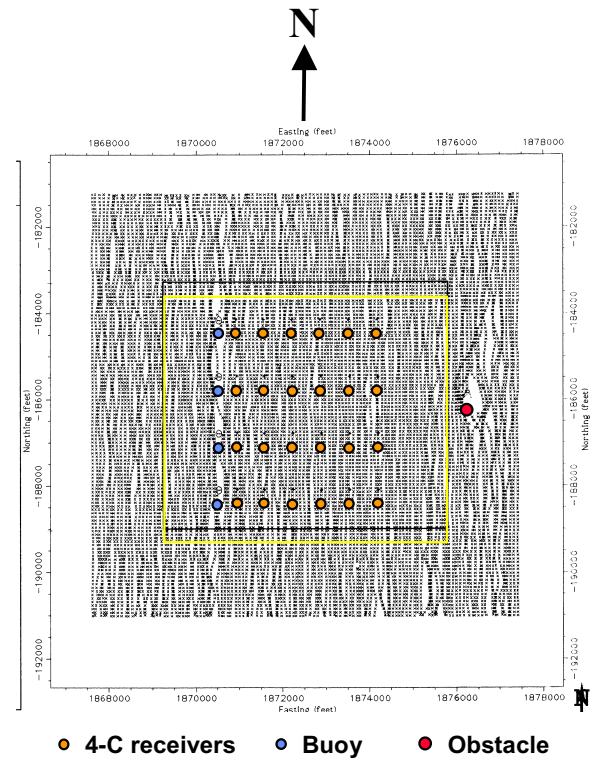


Figure 1. Map view of source grid, superimposed on receiver layout. Sail lines for the source boat run north-south.

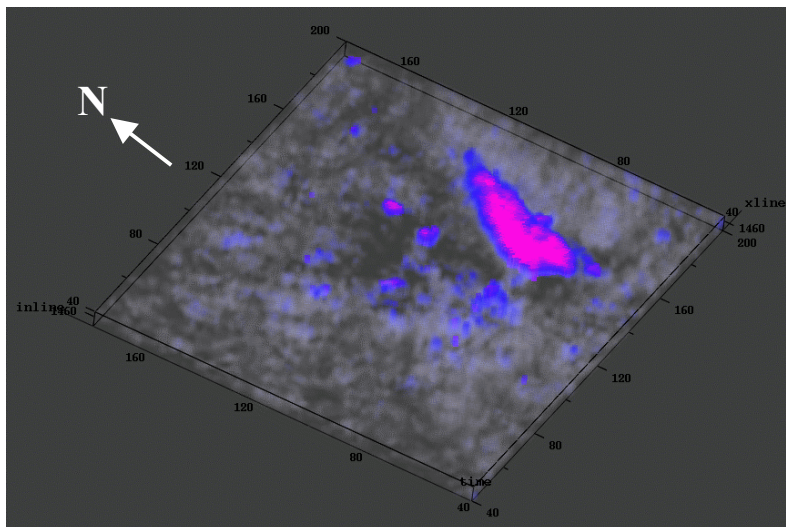
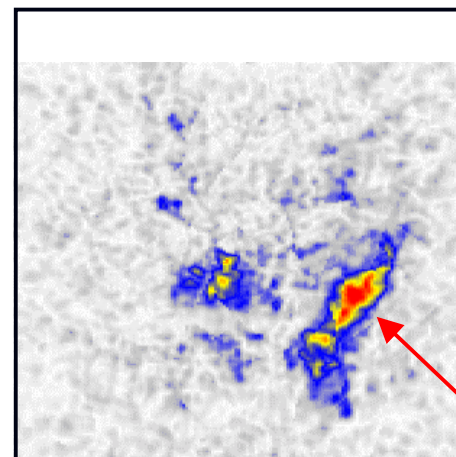
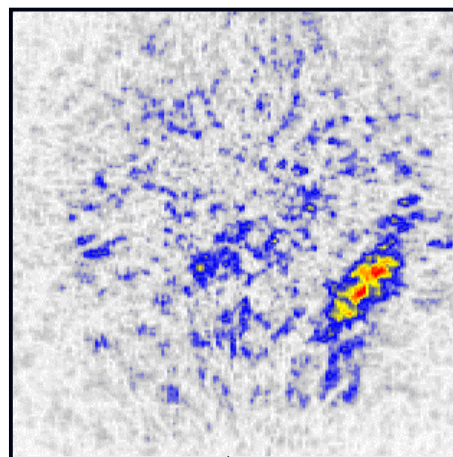
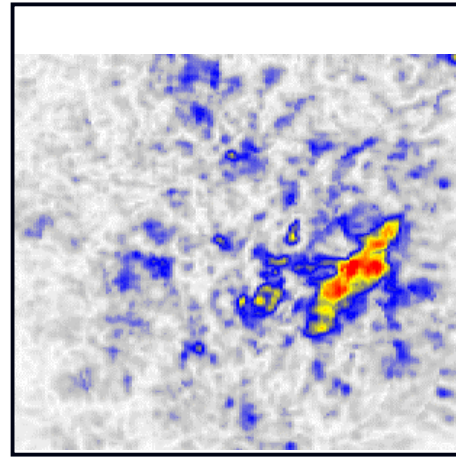
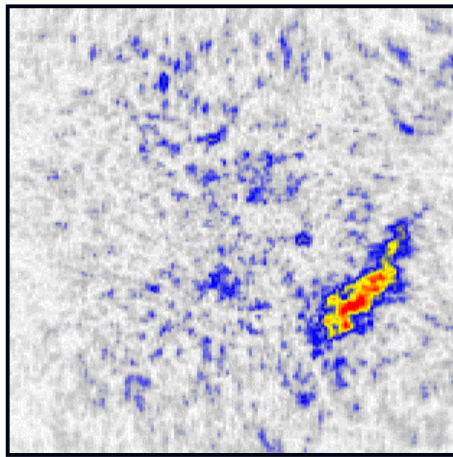
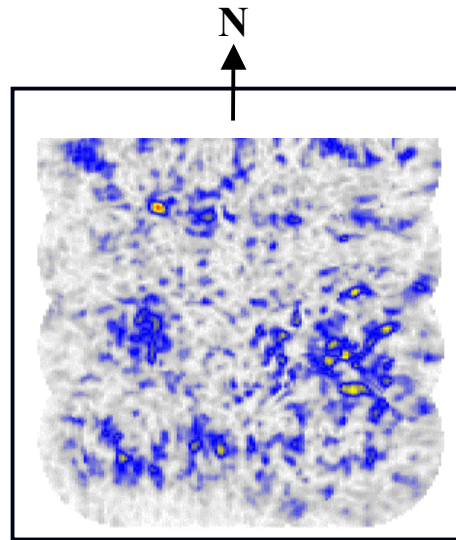
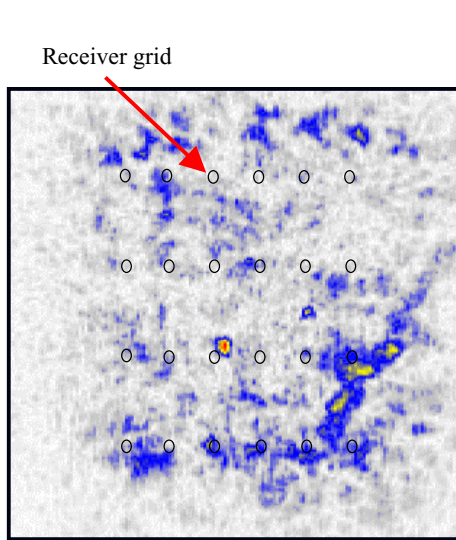


Fig. 4. Volume visualization of the fluid-factor anomaly associated with one of the productive sands. The anomaly is consistent with known pay in one reservoir compartment, and terminates updip (to the SE) against a fault and downdip at the oil-water contact.

Using sparse-receiver data for AVO



Anomaly terminates updip against fault

Fig. 2. Time slices at 1476 ms through poststack-time-migrated near-, mid-, and far-range stacks.

Fig. 3. Time slices at 1476 ms through near-, mid-, and far-range stacks of image traces output from common-receiver (prestack) migration.